ISSN 2616-5805 Vol. 5, Issue 2: 25-31, DOI: 10.25236/AJMS.2024.050205

A Multi Beam Sounding Model Based on Greedy Algorithm and Goal Planning

Shiquan Wen[1], Liting Li[1,*], Jiachao Xia[1], Yuanying Liu[1], Ning Wang[1,2]

[1]*Xiamen Huaxia University, Xiamen, 361024, China*
[2]*A New Generation of Information Communication Technology and Wisdom Education Fujian Engineering Research Center, Xiamen, 361024, China*
[*]*Corresponding author: Lilt@hxxy.edu.cn*

Abstract: *This article first constructs a mathematical model in two-dimensional space that accounts for the distance between the measuring line and the initial point, the depth of seawater, the coverage width, and the overlap rate. Then, applying the principles of spatial geometry, it establishes a three-dimensional model for multi-beam coverage width. Finally, addressing the complexity of actual sea areas, a goal planning model is constructed to minimize the total length of survey lines, utilizing regional division and greedy algorithms.*

Keywords: *Multi beam depth measurement, Least squares method, Goal planning type, Greedy Algorithm*

1. Introduction

The multi-beam ocean sounding system[1][2], a key technology in marine geological research, provides more detailed seabed terrain data than single-beam technology. While multi-beam technology has achieved full coverage measurements in flat seabed areas, there remains scope for improving efficiency and accuracy in complex terrains and diverse marine environments.

2. Establishment and analysis of a two-dimensional detection model

In two-dimensional space, a geometric triangulation model is established based on the angle between the multi-beam plane and the seabed slope, as well as the varying seawater depth along the measuring line from the initial point. Utilizing the sine theorem, a mathematical model is formulated that relates the distance d_i(i =1, 2, 3,...) , seawater depth D_i, coverage width W_i, and the overlap rate of adjacent bands.

2.1 Analysis of seawater depth and measurement line distance

As shown in Figure 1, emitted multi-beam echoes produce varying height differences at different distances. A geometric triangle model, constructed from this, determines the mathematical relationship between seawater depth variance and the spacing of survey lines.

$$D_{i+1} = D_i - d_i \tan\alpha \tag{1}$$

In this model, D_0 represents the depth of seawater at the initial point, and α denotes the slope of the sea surface.

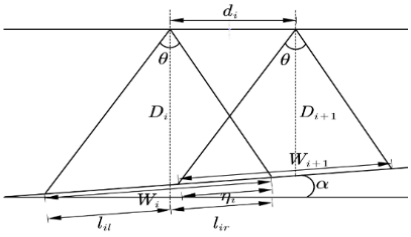

Figure 1: Schematic diagram of multi beam detection

ISSN 2616-5805 Vol. 5, Issue 2: 25-31, DOI: 10.25236/AJMS.2024.050205

2.2 Solving for coverage width

The overlap ratio between coverage width and adjacent bands is shown in Figure 1. Let the left beam coverage width of the i-th measuring line be l_{il}, and the right l_{ir}. Derive the depth of seawater D_i from the sine theorem, along with the beam coverage widths l_{il}, l_{ir}, the slope angle on both sides α, and the opening angle of the multi-beam transducer θ. The relationship between these variables is

$$\begin{aligned} \frac{l_{il}}{\sin\left(\frac{\theta}{2}\right)} &= \frac{D_i}{\sin\left(90^\circ - \frac{\theta}{2} - \alpha\right)} \\ \frac{l_{ir}}{\sin\left(\frac{\theta}{2}\right)} &= \frac{D_i}{\sin\left(90^\circ - \frac{\theta}{2} + \alpha\right)}. \end{aligned} \tag{2}$$

The sum of l_{il} and l_{ir} under a certain multi beam detection can represent the coverage width W_i of the current multi beam on the slope, and the coverage width formula can be obtained

$$W_i = \frac{D_i \sin\theta \cos\alpha}{\cos\left(\alpha + \frac{\theta}{2}\right)\cos\left(\alpha - \frac{\theta}{2}\right)}. \tag{3}$$

2.3 Overlap rate of adjacent detection bands

Given the formula for the overlap rate between adjacent strips with parallel measuring lines when the seabed terrain is flat, a general definition formula for the overlap rate of adjacent strips needs to be derived in the case of slopes. Let the overlapping coverage width of adjacent strips on the slope be n, the width of the non overlapping part be m, and the sum of the two is W_i, as shown in Figure 2.

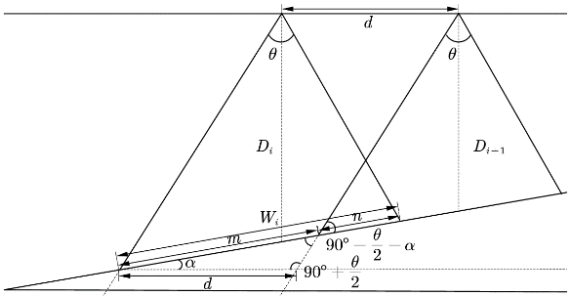

Figure 2: Diagram of Overlap Rate on Slope

According to the properties of parallelograms and the sine theorem, it can be concluded that

$$\frac{m}{\sin\left(90^\circ + \frac{\theta}{2}\right)} = \frac{d}{\sin\left(90^\circ - \frac{\theta}{2} - \alpha\right)}. \tag{4}$$

So the general definition of adjacent overlap rate is obtained, where, when η_i<0 , it indicates missed measurement.

$$\eta_i = \begin{cases} 1 - \dfrac{d * \sin\left(90^\circ + \frac{\theta}{2}\right)}{W_i * \sin\left(90^\circ - \frac{\theta}{2} - \alpha\right)} & i = 2, 3, 4, \ldots \\ 0, & i = 1 \end{cases} \tag{5}$$

3. Construction and characteristics of 3D detection models

When analyzing three-dimensional sea areas, it is found that the angle formed by the intersection of

ISSN 2616-5805 Vol. 5, Issue 2: 25-31, DOI: 10.25236/AJMS.2024.050205

the survey line and the seabed plane changes with different sailing directions. By applying principles of spatial geometry, we can deduce the mathematical relationship between β (the survey line direction angle) and α (the seabed slope angle). Additionally, a model has been developed to determine the coverage width of survey vessels under various sea depths and survey line directions.

3.1 Analysis of Line Surface Angles in Different Measurement Line Directions

In three-dimensional sea area analysis, the multibeam survey line plane is perpendicular to both the survey direction and the seabed plane. It intersects with the seabed slope to form a line of intersection, which determines the width of the beam coverage. The extension of this line of intersection meets the seabed plane at an angle, denoted as φ (the line-plane angle). The angle between the projection of the survey direction and the normal to the seabed slope on the horizontal plane is called β (referred to as the survey line direction angle), as illustrated in Figure 3. When β is 90° or 270°, φ is equal to α (the seabed slope angle). Otherwise, φ varies with changes in β.

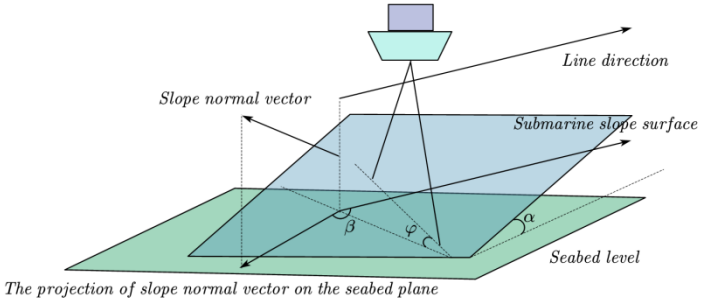

Figure 3: Schematic diagram of line surface angle

Establish a spatial Cartesian coordinate system with the projection of the initial point of the sea area on the seabed plane as the origin O. Let the length of the area to be measured be *c*, the width be *a*, and the height of the intersection point *B* between the slope and the Z-axis be *b*. Let C be the intersection point of the measurement line plane and the slope intersection line on the seabed plane. Using coordinates A(0, a, 0), B(0, 0, b), and C(c, a, 0), along with the normal vectors $\vec{m}$ on the seabed slope and β, the corresponding angle between the intersection line and the survey line plane is proven to be $\varphi=\varphi'$ by filling the slope surface with the seabed plane into a rectangular prism (as shown in Figure 4) and utilizing the spatial symmetry of the prism.

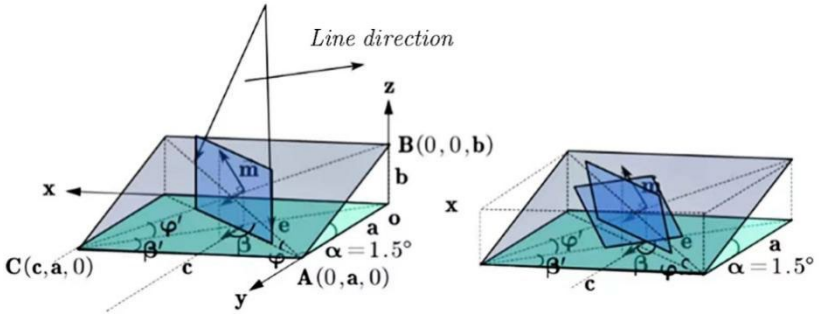

Figure 4: Spatial Cartesian Coordinate System Diagram of Slope Surface

An analysis was conducted on the three surfaces of AoB, AoC, and BoC to determine the relationship between slope angle, measurement line direction angle, and line surface angle. On this basis, derive a description of the line surface angle in any measuring line direction φ Expression for

$$\tan\varphi = \tan\alpha \cdot |\cos\beta| \tag{6}$$

Specifically, when the direction of the measuring line forms an angle β of 90° or 270° with the horizontal plane, the angle φ is equal to the seabed slope angle α. Conversely, when β is at 0° or 180°, the intersection line between the measuring line plane and the slope surface does not extend to the seabed plane.

ISSN 2616-5805 Vol. 5, Issue 2: 25-31, DOI: 10.25236/AJMS.2024.050205

3.2 Establishment of a three-dimensional multi beam coverage width model

As shown in Figure 5, analyze the relationship between the distance between any two measuring lines and the corresponding depth of seawater.

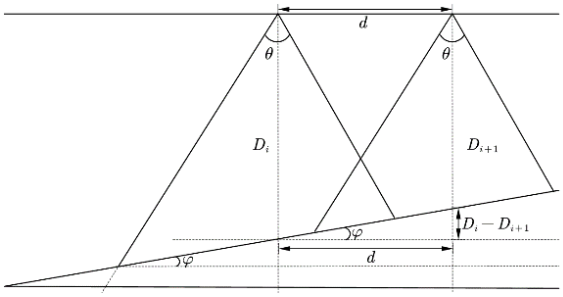

Figure 5: Relationship diagram between measurement line spacing and seawater depth

Establish a mathematical relationship between the distance between survey lines and the depth difference of seawater based on the similarity property of triangles

$$\tan\varphi = \frac{D_i - D_{i+1}}{d} \tag{7}$$

Based on a two-dimensional model, extend to three-dimensional space and derive a formula for calculating seawater depth

$$\begin{aligned} D_i &= D_0 - d_i\tan\varphi \quad (90° < \beta < 270°) \\ D_i &= D_0 + d_i\tan\varphi \quad (else) \end{aligned} \tag{8}$$

Similarly, derive a three-dimensional multi beam coverage width model

$$W_i = \frac{D_i\sin\theta\cos\left(\arctan\left(\tan\alpha\cdot|\cos\beta|\right)\right)}{\cos\left(\arctan\left(\tan\alpha\cdot|\cos\beta|\right)+\frac{\theta}{2}\right)\cos\left(\arctan\left(\tan\alpha\cdot|\cos\beta|\right)-\frac{\theta}{2}\right)} \tag{9}$$

4. The Application of Greedy Algorithm and Target Planning in Marine Exploration Models

For a certain actual sea area, to achieve full coverage, the shortest total length of survey lines, and to meet the overlap rate, this paper proposes a measurement scheme that integrates a greedy algorithm with target planning[3][4]. A planning model with the optimization objective of minimizing the length of survey lines is created by analyzing and zoning the sea area using a three-dimensional exploration model. The model employs greedy algorithms to find the optimal path within each partition, thereby achieving global optimization of the survey line path.

4.1 Determine the optimal navigation direction

Considering spatial symmetry, the navigation direction angle is set at [0 °, 180 °]. Establish a functional relationship between the length l_i of the measuring line and the coverage width W_i through a 3D model

$$S = \sum_{i=1}^{n} l_i \cdot \frac{D_i\sin\theta\cos\left(\arctan\left(\tan\alpha\cdot|\cos\beta|\right)\right)}{\cos\left(\arctan\left(\tan\alpha\cdot|\cos\beta|\right)+\frac{\theta}{2}\right)\cos\left(\arctan\left(\tan\alpha\cdot|\cos\beta|\right)-\frac{\theta}{2}\right)} \tag{10}$$

To maximize coverage width while minimizing the total length of survey lines, with the sea area remaining constant, the optimal navigation direction is determined by comparing coverage widths across different navigation directions, thereby minimizing the survey line length. Given the sea area slope α, the transducer opening angle θ, and the initial sea depth D_0, Figure 6 illustrates the functional relationship between the survey line direction β and the coverage width W_i.

ISSN 2616-5805 Vol. 5, Issue 2: 25-31, DOI: 10.25236/AJMS.2024.050205

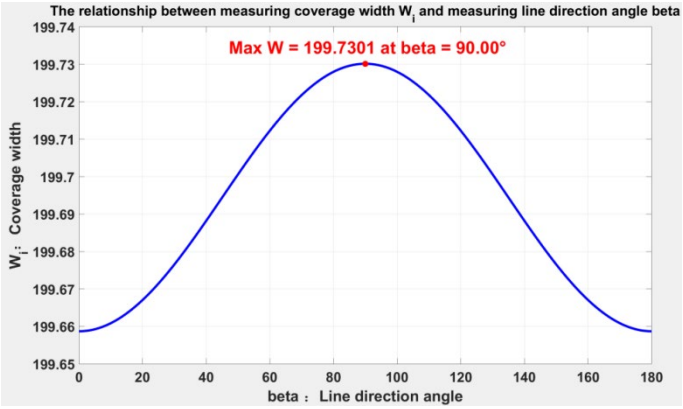

Figure 6: Line direction β Relationship diagram with coverage width Wi function

Analyzing Figure 6, it can be concluded that the optimal measurement effect can be achieved and the total length of the survey line can be minimized when the exploration vessel is heading at 90°, that is, when the survey line is parallel to the seabed contour line.

4.2 Sea area zoning processing

In response to the measurement challenges caused by the large terrain fluctuations in actual sea areas, this study adopts a regional planning strategy to simplify calculations and improve fitting results. Based on the contour map, divide the sea area into multiple small areas and plan each area independently. Using the previously established method for detecting flat slope sea areas, convert irregular sea areas into flat slope models for analysis and calculation.

In a spatial Cartesian coordinate system, the seabed slope equation $z=ax+by+c$ is fitted using the least squares method to evaluate the sum of squared residuals between the fitted depth and the measured values, and to determine the angle between the slope and the seabed plane. The relevant results are summarized in Table 1.

Table 1: Fitting plane equations and parameters for each partition area

partition	From west to east		From south to north		Fit the plane equation Z	Sum of squared residuals	Slope angle °
region 1	0	2	3.5	5	0.800x+22.112y-28.688	9326.58	2.59
region 2	2	3.24	3.5	5	3.392x + 9.195y + 21.354	24070.35	5.83
region 3	3.24	4	3.5	5	4.992x -7.312y + 86.449	12441.34	6.44
region 4	3	4	1.76	3.5	35.904x -15.445y + 4.676	40491.07	1.47
region 5	3	4	0	1.76	69.504x -26.645y -93.248	44603.20	0.77
region 6	2	3	1.76	3.5	23.936x + 0.555y -1.500	19931.76	2.39
region 7	2	3	0	1.76	46.336x -10.645y -37.825	23334.80	1.20
region 8	1	2	1.76	3.5	11.968x + 10.155y -2.812	7597.11	3.65
region 9	1	2	0	1.76	23.168x -1.045y + 0.063	10573.34	2.65
region 10	0	1	1.5	3.5	0.000x + 12.523y + 3.136	6251.38	4.57
region 11	0	0.5	0	1.5	-6.000x + 1.328y + 22.340	737.62	9.24
region 12	0.5	1	0	1.5	6.000x + 1.328y + 16.340	737.62	9.24

And based on this, draw a 3D fitting plan of the sea area, as shown in Figure 7.

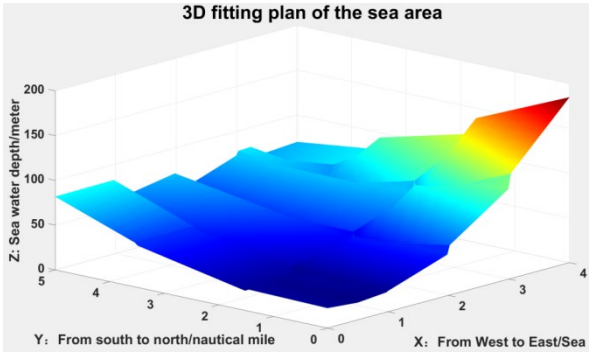

Figure 7: 3D fitting plan of the sea area

ISSN 2616-5805 Vol. 5, Issue 2: 25-31, DOI: 10.25236/AJMS.2024.050205

4.3 Construction of Multi beam Sounding Model Based on Greedy Algorithm and Goal Planning

In the marine exploration model, the greedy algorithm selects the optimal path at each step, applying the greedy algorithm[5] to each area for local optimization. Local optimal solutions are then integrated to form the optimal exploration plan for the entire marine area.

After setting the heading and dividing the sea area, the measurement plan was refined. With survey lines parallel to seabed contour lines and each set to length Lh, the complex two-dimensional coverage problem is simplified to an optimization of one-dimensional line segment accumulation. This is further transformed into calculating the required number of measuring lines i in the LV direction for comprehensive coverage. Survey lines are arranged from deep to shallow, as shown in Figure 8.

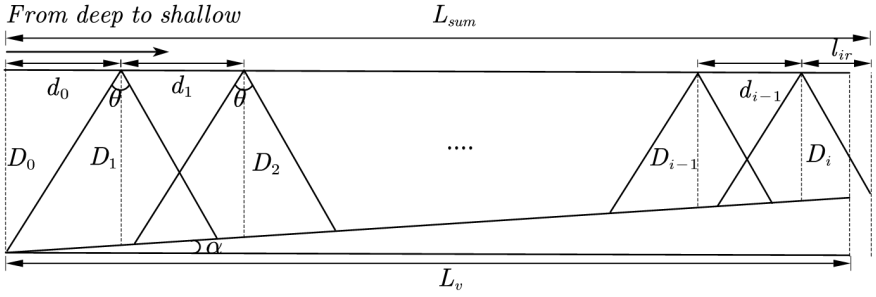

Figure 8: Layout of survey lines from deep to shallow

1) Initialization: Starting from the deepest point D_0 in each sea area zone, the first measuring line is connected to the depth D_1 of the seawater at that point with an interval of d_0.

2) Local optimal strategy: Starting from the starting point, based on the current sea slope and survey line direction, gradually expand the survey line path from deep to shallow, and construct a goal planning model that minimizes the total length L_{sum} of the survey line while meeting the coverage width L_v requirements of each area:

$$\min\ L_{sum} = d_0 + \sum_{i=1}^{n} d_i + l_{ir}$$

$$s.t.\begin{cases} W_i = \dfrac{D_i \sin\theta\cos\alpha}{\cos\left(\alpha+\frac{\theta}{2}\right)\cos\left(\alpha-\frac{\theta}{2}\right)} \\ \eta_{i\min} \leqslant 1 - \dfrac{d_i * \sin\left(90^\circ+\frac{\theta}{2}\right)}{W_i * \sin\left(90^\circ-\frac{\theta}{2}-\alpha\right)} \leqslant \eta_{i\max} \\ l_{ir} = \dfrac{D_i \sin\left(\frac{\theta}{2}\right)}{\sin\left(90^\circ-\frac{\theta}{2}+\alpha\right)} \\ D_{i+1} = D_0 + \sum_{i=0}^{n} d_i \tan\alpha \\ L_{sum} \geqslant L_v \end{cases} \tag{11}$$

3) Subproblem solving: iteratively calculate the survey line paths within the community until the entire community is covered, and obtain the number of survey lines *i* under the current survey line layout. And modify the position of the first measuring line, iteratively solve it repeatedly, and form a local optimal solution. The flowchart is shown in Figure 9.

ISSN 2616-5805 Vol. 5, Issue 2: 25-31, DOI: 10.25236/AJMS.2024.050205

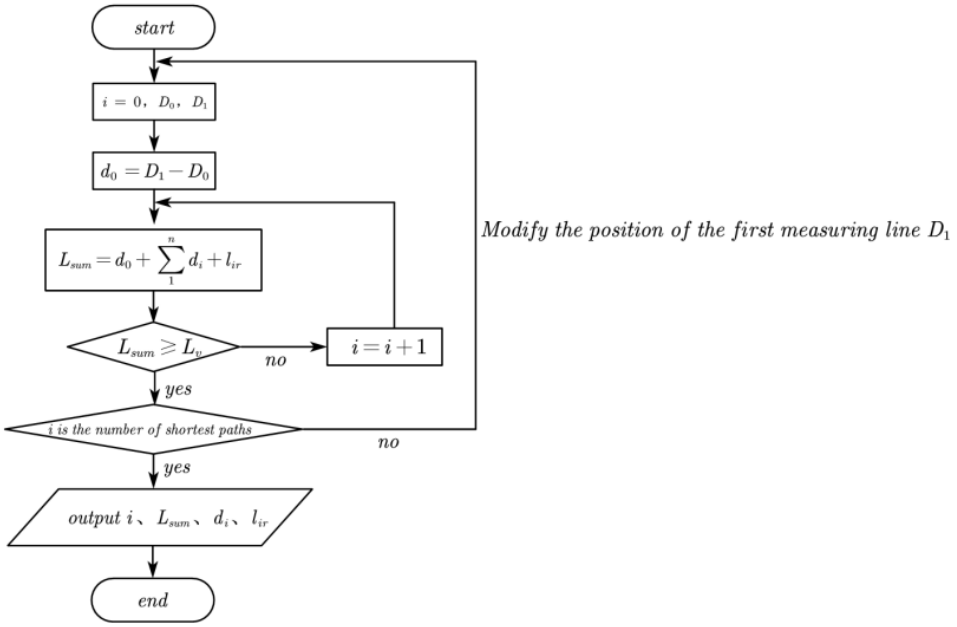

Figure 9: Model Calculation Flowchart

4) Local optimal solution integration: Integrate the optimal solutions of various subproblems, globally optimize survey lines to eliminate overlapping areas and fill in missing measurement areas.

In summary, the calculated total length of the survey line is 261,879.69 meters, with a minimal 0.14% of areas missed. Additionally, there is a segment of 3,409.11 meters where the survey line has an overlap rate exceeding 20%.

The mathematical model, which combines goal planning with the greedy algorithm, offers an efficient means to balance global optimization with local path efficiency. Enhanced by three-dimensional geometric modeling, it adapts well to complex seabed terrain, providing an economical and flexible optimization path for ocean exploration.

References

[1] Jiang Y, Yang Z, Liu Z, et al. High-resolution bottom detection algorithm for a multibeam echo-sounder system with a U-shaped array [J]. Acta Oceanologica Sinica, 2018, 37(7):78-84.
[2] Karadeniz S K, Rıfat H, Sedar K G, et al. Modeling and Analysis of Sea-Surface Vehicle System for Underwater Mapping Using Single-Beam Echosounder[J].Journal of Marine Science and Engineering, 2022, 10(10):1349-1371.
[3] Zardashti R, Nikkhah A, Yazdanpanah M .Multi-objective trajectory planning over terrain using label-setting greedy-based algorithm [J].Proceedings of the Institution of Mechanical Engineers, Part G: Journal of Aerospace Engineering, 2015, 229(8):1435-1453.
[4] Ilham G S, Endang S, Alamsyah A .Comparison of Dynamic Programming Algorithm and Greedy Algorithm on Integer Knapsack Problem in Freight Transportation[J].Scientific Journal of Informatics, 2018, 5(1):49-58.
[5] S. K V .Comparison of Purely Greedy and Orthogonal Greedy Algorithm[J].Mathematical Notes, 2024, 115(1-2):37-43.